
**Liquid Crystals**
Publication details, including instructions for authors and subscription information:
http://www.informaworld.com/smpp/title~content=t713926090

# Synthesis and characterisation of thermotropic liquid-crystalline properties of azomethine dimers

Pradip K. Bhowmik[a]; Haesook Han[a]; Alexi K. Nedeltchev[a]; Hari D. Mandal[b]; Jose A. Jimenez-Hernandez[b]; Patrick M. McGannon[b]; Leonardo Lopez[b]; Shin-Woong Kang[c]; Satyendra Kumar[c]
[a] Department of Chemistry, University of Nevada at Las Vegas, Las Vegas, NV, USA [b] Department of Biology and Chemistry, Texas A&M International University, 5201 University Boulevard, Laredo, TX, USA [c] Department of Physics, Kent State University, Kent, OH, USA

Online publication date: 14 December 2009

**To cite this Article** Bhowmik, Pradip K. , Han, Haesook , Nedeltchev, Alexi K. , Mandal, Hari D. , Jimenez-Hernandez, Jose A. , McGannon, Patrick M. , Lopez, Leonardo , Kang, Shin-Woong and Kumar, Satyendra(2009) 'Synthesis and characterisation of thermotropic liquid-crystalline properties of azomethine dimers', Liquid Crystals, 36: 12, 1389 — 1399
**To link to this Article: DOI:** 10.1080/02678290903229585
**URL:** http://dx.doi.org/10.1080/02678290903229585

*Liquid Crystals,*
Vol. 36, No. 12, December 2009, 1389–1399

Taylor & Francis
Taylor & Francis Group

# Synthesis and characterisation of thermotropic liquid-crystalline properties of azomethine dimers

Pradip K. Bhowmik[a]*, Haesook Han[a], Alexi K. Nedeltchev[a], Hari D. Mandal[b], Jose A. Jimenez-Hernandez[b], Patrick M. McGannon[b], Leonardo Lopez[b], Shin-Woong Kang[c] and Satyendra Kumar[c]

[a]*Department of Chemistry, University of Nevada at Las Vegas, 4505 Maryland Parkway, Box 454003, Las Vegas, NV 89154, USA;* [b]*Department of Biology and Chemistry, Texas A&M International University, 5201 University Boulevard, Laredo, TX 78041, USA;* [c]*Department of Physics, Kent State University, Kent, OH 44242, USA*

*(Received 2 July 2009; final form 3 August 2009)*

A series of azomethine dimers were prepared by condensation reactions of benzaldehyde, biphenylcarboxaldehyde and 9-anthraldehyde with various aromatic diamines of varying flexibility in ethanol in the presence of tosic acid. Their chemical structures were determined by Fourier transform infrared and $^{1}H$ and $^{13}C$ nuclear magnetic resonance (NMR) spectroscopies, as well as elemental analysis. Their thermal properties were also examined by using a number of experimental techniques, including differential scanning calorimetry (DSC), thermogravimetric analysis (TGA), polarising optical microscopy (POM) and variable temperature X-ray diffraction (VTXRD). Azomethine dimer, prepared from benzaldehyde and 1,9-bis(4-aminophenoxy)nonane, exhibited a monotropic, nematic liquid-crystalline (LC) phase. The majority of the azomethine dimers containing biphenyl moieties exhibited enantiotropic, nematic LC phase on melting at relatively low temperatures, since they developed typical Schlieren, threaded or marbled textures in their LC phase. They also had accessible isotropisation temperatures well below their decomposition temperatures. Azomethine dimers containing anthracene moieties did not exhibit LC properties, but exhibited polymorphism as determined by POM and VTXRD in two cases. All of these azomethine dimers in the series had excellent thermal stability that was in the broad range of temperatures of 307–400°C depending on their degrees of aromaticity index.

**Keywords:** azomethine dimers; synthesis; thermotropic; liquid-crystalline phase; nematic; Schlieren texture



## 1. Introduction

Azomethine is an important functional group in both organic and polymer chemistry, which is generally produced by the reaction of an aldehyde and a primary amine in presence of an acid catalyst. This key functional group is the basis of forming a large number of both rod-like and banana-shaped like mesogens forming thermotropic liquid-crystalline (LC) compounds. In addition, suitably designed organic compounds, including heterocyclic compounds or polymers containing azomethine linkages, exhibit high thermal stability, semiconducting properties and the ability to form organometallic complexes (*1–10*). Henderson *et al.* (*4*) reported the results of thermotropic LC properties of a large number of azomethine LC dimers. For example, the dimers, prepared from both *p*-methyl-benzaldehyde and *p*-ethyl-benzaldehyde with 1,3-bis(aminophenoxy)propane (BAPP), do not form a LC phase on melting. In contrast, dimers of these two aldehydes with 1,4-bis(aminophenoxy)butane (BAPB) exhibit an enantiotropic nematic LC phase on melting and have mesophase ranges of 10 and 12°C, respectively. The dimers, prepared from BAPP and BAPB with biphenylcarboxaldehyde, also exhibited a nematic LC phase on melting. In addition, the dimer from BAPP has a mesophase range of 13°C and that from BAPB has a nematic-to-isotropic transition ($T_i$) near to its decomposition temperature that precluded the determination of both $T_i$ and the mesophase range. In addition, dimers prepared from these two diamines with 1-pyrenecarboxaldehyde do not form a thermotropic LC phase, but instead exhibit complex thermal properties in their differential scanning calorimetry (DSC) studies (*4*).

In this article, we describe the synthesis of a series of azomethine dimers (**1–14**, see Scheme 1), prepared from the condensation reactions of two equivalents of appropriate aldehydes with the corresponding aromatic diamines in ethanol in the presence of an acid catalyst, and the characterisation of their chemical structures by using various spectroscopic techniques and elemental analyses. Their thermotropic LC properties were examined by using various experimental techniques with the aim of understanding the structure–property relationships and developing novel materials based on this class of compounds.

## 2. Experimental

### 2.1 Materials

Benzaldehyde, biphenylcarboxaldehyde, 9-anthraldehyde, 1,6-dibromohexane, 1,9-dibromononane, ethylene

*Corresponding author. Email: pradip.bhowmik@unlv.edu

This article is dedicated to Professor Timothy C.K. Su with best wishes on the occasion of his 65th birthday.

ISSN 0267-8292 print/ISSN 1366-5855 online

DOI: 10.1080/02678290903229585
http://www.informaworld.com

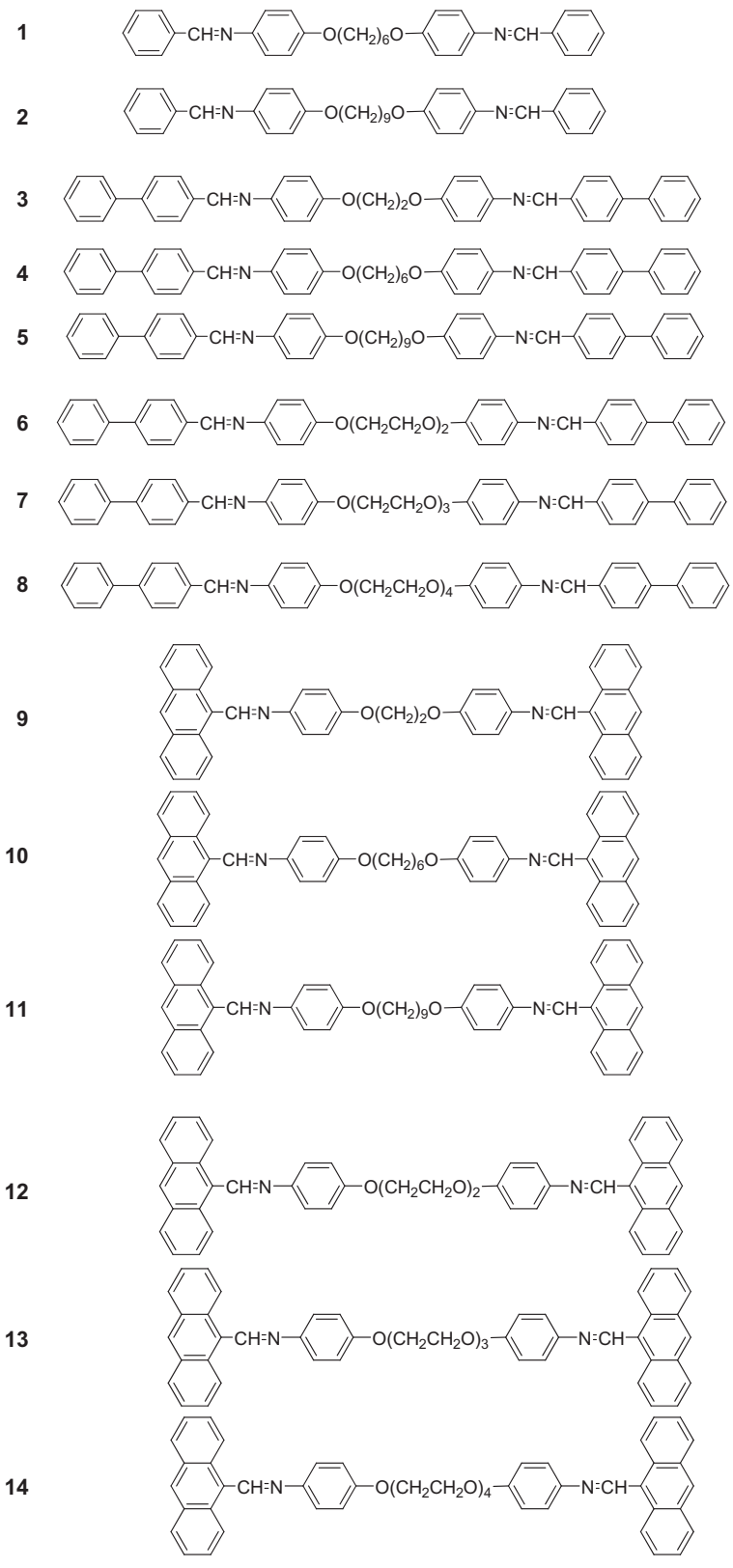


Scheme 1. Chemical structures of synthesised azomethine dimers **1–14**.

glycol, diethylene glycol, triethylene glycol, tetraethylene glycol, 1-fluoro-4-nitrobenzene, potassium carbonate, tosic acid, hydrazine monohydrate, ethanol, toluene and N,N-dimethylformamide (DMF) were purchased from Alpha Aesar and used as received for the synthesis of various intermediates and azomethine dimers.

### 2.2 Synthesis of aromatic diamines

The two aromatic diamines, 1,6-bis(4-aminophenoxy)hexane (BAPH) and 1,9-bis(4-aminophenoxy)nonane (BAPN), were prepared in two steps from acetamidophenol according to the procedure described in the literature (*4*). The first step was the reaction of acetamidophenol with the desired α,ω–dibromoalkane in acetone in the presence of potassium carbonate on heating to reflux. The product was then acid hydrolysed, followed by neutralisation reaction to afford the desired diamine. Both of the aromatic diamines were then recrystallised from toluene. BAPH exhibited a crystal-to-crystal transition at 108°C and a crystal-to-liquid transition ($T_m$) at a peak maximum of 144°C, along with an indistinct shoulder peak in the low temperature region as determined by DSC at a heating rate of 10°C min$^{-1}$ in nitrogen. In the second heating cycle, its crystal-to-crystal transition peak was shifted slightly to a higher temperature of 127°C and the melting peak maximum was shifted slightly at the lower temperature of 142°C. BAPN had a melting peak maximum at 80°C in the first heating cycle, but it had a melting peak maximum at 79°C along with a crystal-to-crystal transition peak at 68°C in the second heating cycle. However, the literature-reported m.p. values were 117 (*11*) or 144 (*12*) and 75 (*12*) or 80–82°C (*13*), respectively. The other four aromatic diamines, 1,2-bis(4-aminophenoxy)ethane (BAPE), bis(2-(4-aminophenoxy)ethyl) ether (BAPDiEO, hereafter DiEO), 1,2-bis(2-(4-aminophenoxy)ethyoxy)ethane (BAPTriEO, hereafter TriEO) and bis(2-(2-(4-aminophenoxy)ethoxy)ethyl) ether (BAPTetraEO, hereafter TetraEO), were also prepared in two steps from 1-fluoro-4-nitrobenzene according to the known procedures (*11*). The first step was the reaction 1-fluoro-4-nitrobenzene with the appropriate aliphatic diols in the presence of potassium carbonate in DMF on heating to reflux to produce the corresponding dinitroderivatives of the desired chemical structures, which were subsequently reduced to the desired diamines with hydrazine monohydrate in ethanol in the presence of 10% Pd C$^{-1}$ on heating to reflux. The first diamine (BAPE) was recrystallised from water and the other two diamines (DiEO and TriEO) were purified by recrystallisation from ethanol. Their melting peak maxima, from the thermograms as determined by DSC at a heating rate of 10°C min$^{-1}$ in nitrogen, were found to be at 179, 64 and 95°C and their literature m.p. values were 176 (*14*) or 179–180 (*15*), 59–60 (*15*) and 93–95°C (*15*), respectively. The fourth aromatic diamine (TetraEO) was obtained as viscous liquid from the reaction mixture and further purified by passing through silica-gel column chromatography using chloroform as an eluent.

### 2.3 Synthesis of azomethine dimers 1–14

All of these dimers were essentially prepared by using an identical procedure of an acid-catalysed condensation reaction of two equivalents of aldehydes with the aromatic diamines and, therefore, a representative procedure for the preparation of **1** is described below. In a round-bottomed flask were placed a magnetic stirring bar, 1,6-bis(4-aminophenyl-1-oxy)hexane (5.1 g, 0.017 mol), ethanol (50 ml), and a few crystals of *p*-toluenesulfonic acid. The mixture was heated to reflux and benzaldehyde (4.0 g, 0.038 mol) was slowly added to the stirred, boiling solution. The mixture was heated under reflux for an additional 3 h. The solution was cooled, resulting in the precipitation of product, which was then collected by vacuum filtration and washed with cold ethanol. The crude product (6.87 g, 85%) was recrystallised from toluene. $^1$H nuclear magnetic resonance (NMR) (400 MHz, *d6*-dimethylsulfoxide (DMSO), 368° K): $\delta$ (ppm) 8.60 (s, C<u>H</u>=N, 2H), 7.47–7.90 (m, phenyl, 10H), 7.24–7.26 (d, $J = 8.8$ Hz, 4H), 6.95–6.70 (d, $J = 8.8$ Hz, 4H), 4.02 (t, $J = 6.6$ Hz, 4H), 1.77 (m, 4H), 1.52 (m, 4H). $^{13}$C NMR (100 MHz, *d6*-DMSO, 368 K): $\delta$ (ppm) 158.89, 158.59,158.29, 145.09, 137.28, 131.78, 131.28, 129.56, 129.07, 128.91, 123.15, 122.62, 116.18, 116.21, 115.92, 68.82, 29.42, 25.96. Note here that it showed three carbon signals of azomethine carbon instead of a single carbon signal in its $^{13}$C NMR spectrum. In addition, its total number of carbon signals was greater than that of the assigned chemical structure. These results suggested that it existed in solution in various populated conformations of two azomethine linkages, such as cis–cis, cis–trans and trans–trans. Elemental analysis: calculated (found) for $C_{32}H_{32}N_2O_2$ (476.63), 80.64 (80.30), H 6.77 (7.10), N 5.88 (6.39). Data for **2**: Yield 88% (recrystallised from toluene). Infrared (IR) (KBr, $\nu_{max}$ cm$^{-1}$): 3092, 3055, 3034 (C–H stretching of the aromatic rings), 2928, 2874, 2849, 2761 (C–H stretching of the aliphatic chains), 1900, 1621 (CH=N stretching), 1502, 1469, 1290, 1250, 1191, 1112, 1070, 1012 (C–O–C stretching), 969, 834, 752, 686 (C–H oop bending of the aromatic rings). $^1$H NMR (400 MHz, *d6*-DMSO, 368 K): $\delta$ (ppm) 8.58 (s, C<u>H</u>=N, 2H), 7.46–7.90 (m, phenyl, 10H), 7.22–7.24 (d, $J = 6.4$ Hz, 4H), 6.93–6.95 (d, $J = 6.8$ Hz, 4H), 3.97–4.00 (t, $J = 6.6$ Hz, 4H), 1.69–1.76 (m,

4H), 1.35–1.45 (m, 10H). $^{13}$C NMR (100 MHz, *d6*-DMSO, 368 K): $\delta$ (ppm) 158.82, 158.53, 158.30, 145.06, 137.26, 131.74, 131.27, 129.50, 129.09, 128.90, 123.10, 122.66, 116.12, 115.92, 69.10, 68.87, 68.66 29.46, 29.27, 26.13 (*vide supra*, Figure S1, which is available via the multimedia link on the online article webpage). Elemental analysis: calculated (found) for $C_{35}H_{38}N_2O_2$ (518.71), 81.05 (81.29), H 7.38 (7.25), N 5.40 (5.51). Data for **3**: Yield 93% (recrystallised from DMF). Elemental analysis: calculated (found) for $C_{40}H_{52}N_2O_2$ (572.17), 83.89 (83.81), H 5.63 (6.00), N 4.89 (4.97). Data for **4**: Yield 94% (recrystallised from DMF). Elemental analysis: calculated (found) for $C_{44}H_{40}N_2O_2$ (628.82), 84.04 (83.70), H 6.41 (6.73), N 4.45 (4.63). Data for **5**: Yield 92% (recrystallised from DMF). IR (KBr, $\nu_{max}$ cm$^{-1}$): 3091, 3057, 3035 (C–H stretching of the aromatic rings), 2924, 2849, 2760 (C–H stretching of the aliphatic chains), 1620 (CH=N stretching), 1501, 1365, 1289, 1253, 1237, 1161, 1114, 1009 (C–O–C stretching), 839, 762, 726, 690 (C–H oop bending of the aromatic rings). A poor quality $^1$H NMR spectrum was recorded even at 95°C due to the insolubility of this compound in $d_6$-DMSO. Elemental analysis: calculated (found) for $C_{47}H_{46}N_2O_2$ (670.90), 84.14 (84.29), H 6.91 (7.08), N 4.18 (4.30). Data for **6**: Yield 92% (recrystallised from DMF). Elemental analysis: calculated (found) for $C_{42}H_{36}N_2O_3$ (616.77), 81.79 (81.72), H 5.88 (6.62), N 4.54 (4.68). Data for **7**: Yield 90% (recrystallised from DMF). Elemental analysis: calculated (found) for $C_{44}H_{40}N_2O_4$ (660.82), 79.97 (79.64), H 6.10 (6.39), N 4.24 (4.39). Data for **8**: Yield 90% (recrystallised from DMF). IR (KBr, $\nu_{max}$ cm$^{-1}$): 3090, 3058, 3034 (C–H stretching of the aromatic rings), 2918, 2863, 2740 (C–H stretching of the aliphatic chains), 1895, 1674, 1616 (CH=N stretching), 1502, 1498, 1447, 1368, 1289, 1248, 1141, 1109, 1061, 1012 (C–O–C stretching), 984, 921, 837, 761, 688 (C–H oop bending of the aromatic rings). Elemental analysis: calculated (found) for $C_{46}H_{94}N_2O_5$ (704.88), 78.38 (78.29), H 6.29 (6.63), N 3.97 (4.11). Data for **9**: Yield 96% (recrystallised from DMF). $^1$H NMR (400 MHz, *d6*-DMSO, 298 K): $\delta$ (ppm) 9.81 (s, C<u>H</u>=N, 2H), 7.56–8.85 (m, monosubstituted anthracene moiety, 18H), 8.17–8.19 (d, $J = 8.0$ Hz, 4H), 7.16–7.18 (d, $J = 8.8$ Hz, 4H), 4.45 (s, –OC<u>H$_2$</u>–, 4H). $^{13}$C NMR (100 MHz, *d6*-DMSO, 298 K): $\delta$ (ppm) 158.48, 158.13, 145.86, 131.59, 130.83, 130.65, 129.63, 127.94, 126.28, 125.72, 123.40, 115.93, 67.46. Elemental analysis: calculated (found) for $C_{44}H_{32}N_2O_2$ (620.76), 85.14 (83.98), H 5.20 (6.18), N 4.51 (5.13). Data for **10**: Yield 99% (recrystallised from DMF). Elemental analysis: calculated (found) for $C_{48}H_{40}N_2O_2$ (678.87), 85.18 (84.42), H 5.96 (6.24), N 4.14 (4.12). Data for **11**: Yield 95% (recrystallised from DMF). IR (KBr, $\nu_{max}$ cm$^{-1}$): 3049 (C–H stretching of the aromatic rings), 2929, 2858, 2767 (C–H stretching of the aliphatic chains), 1616 (CH=N stretching), 1500, 1393, 1288, 1242, 1165, 1032, (C–O–C stretching), 831, 786, 729 (C–H oop bending of the aromatic rings). $^1$H NMR (400 MHz, *d6*-DMSO, 298 K): $\delta$ (ppm) 9.73 (s, C<u>H</u>=N, 2H), 7.44–8.79 (m, monosubstituted anthracene moiety, 18H), 8.10–8.12 (d, $J = 8.0$ Hz, 4H), 7.03–7.05 (d, $J = 8.8$ Hz, 4H), 4.03–4.06 (m, 4H), 1.73–1.80 (m, 4H), 1.38–1.47 (m, 10H). $^{13}$C NMR (100 MHz, *d6*-DMSO, 368 K): $\delta$ (ppm) 158.59, 158.13, 158.01, 145.86, 131.74, 130.81, 130.76, 130.44, 129.54, 128.22, 127.92, 126.31, 125.84, 125.77, 125.75, 125.46, 123.28, 122.78, 116.38, 115.98, 68.96, 29.48, 29.31, 26.17 (*vide supra*). Elemental analysis: calculated (found) for $C_{51}H_{47}N_2O_2$ (719.96), 85.08 (85.45), H 6.38 (6.62), N 3.89 (3.95). Data for **12**: Yield 93% (recrystallised from DMF). $^1$H NMR (400 MHz, *d6*-DMSO, 298 K): $\delta$ (ppm) 9.79 (s, C<u>H</u>=N, 2H), 7.53–8.83 (m, monosubstituted anthracene moiety, 18H), 8.16–8.17 (d, $J = 6.8$ Hz, 4H), 7.10–7.13 (d, $J = 8.4$ Hz, 4H), 4.23 (bs, 4H), 3.90 (bs, 4H). $^{13}$C NMR (100 MHz, *d6*-DMSO, 368 K): $\delta$ (ppm) 158.48, 145.86, 131.57, 129.62, 127.91, 126.25, 125.70, 123.35, 115.89, 68.90, 68.25 (poor quality spectrum). Elemental analysis: calculated (found) for $C_{46}H_{36}N_2O_3$ (664.81), 83.11 (82.74), H 5.46 (6.81), N 4.21 (4.51). Data for **13**: Yield 92% (recrystallised from DMF). Poor quality $^1$H NMR was recorded at room temperature due to the insolubility of this compound in $d_6$-DMSO. Elemental analysis: calculated (found) for $C_{48}H_{40}N_2O_4$ (708.87), 81.33 (80.90), H 5.69 (6.00), N 3.95 (4.34). Data for **14**: Yield 92% (recrystallised from DMF). IR (KBr, $\nu_{max}$ cm$^{-1}$): 3054 (C–H stretching of the aromatic rings), 2923, 2862 (C–H stretching of the aliphatic chains), 1613 (CH=N stretching), 1502, 1449, 1242, 1124, 1047, 1012 (C–O–C stretching), 840, 735 (C–H oop bending of the aromatic rings). $^1$H NMR (400 MHz, *d6*-DMSO, 298 K): $\delta$ (ppm) 9.75 (s, C<u>H</u>=N, 2H), 7.49–8.79 (m, monosubstituted anthracene moiety, 18H), 8.12–8.15 (dd, 4H), 7.06–7.10 (dd, 4H), 4.15–4.17 (m, 4H), 3.79–3.81 (m, 4H), 3.59–3.66 (m, 8H). $^{13}$C NMR (100 MHz, *d6*-DMSO, 298 K): $\delta$ (ppm) 157.47, 157.38, 144.81, 130.97, 130.74, 129.98, 129.80, 128.78, 127.24, 127.06, 125.40, 124.86, 122.51, 115.00, 69.88, 69.78, 68.90, 67.38 (*vide supra*, Figure S2, which is available via the multimedia link on the online article webpage). Elemental analysis: calculated (found) for $C_{50}H_{44}N_2O_5$ (752.92), 79.76 (79.74), H 5.89 (6.31), N 3.72 (3.99).

### *2.4 Characterisation*

IR spectra were recorded with a Shimadzu Fourier transform infrared (FTIR) analyser with neat films

of azomethine compounds on KBr pellets. The $^{1}H$ and $^{13}C$ NMR spectra of several azomethine dimers at both room temperature and high temperature, usually at 95°C whenever possible, were recorded with a Varian nuclear magnetic resonance (VNMR) 400 spectrometer with three radio frequency (RF) channels operating at 400 and 100 MHz, respectively, in *d6*-DMSO using tetramethylsilane (TMS) as an internal standard, since their solubility in the chosen deuterated solvent was rather low at room temperature. Elemental analyses of all of the compounds **1–14** were performed in the NuMega Resonance Laboratories, Inc. (San Diego, California). Phase-transition temperatures were measured with a TA differential scanning calorimeter 910 with a Thermal Analyser 2100 system, calibrated with indium and tin, under a nitrogen flow at heating and cooling rates of 10°C $min^{-1}$, unless otherwise specified. The peak maxima of the endotherms were taken as the transition temperatures. The LC textures, developed in several azomethine dimers, were observed with a polarising optical microscope, Nikon model Labophot 2, equipped with crossed polarisers and a Mettler hot stage. Thermogravimetric analysis (TGA) was performed with TA Instruments equipment with an analyser 2100 system at a heating rate of 10°C $min^{-1}$ under a nitrogen flow. For **10** and **13**, for variable temperature X-ray diffraction (VTXRD) studies, the following procedure was adopted as an example. **10** was loaded into a Lindeman capillary tube, i.e. an unaligned sample, and then loaded into the hot stage, designed for X-ray diffraction (XRD), the diffraction patterns were obtained at different temperatures. It was exposed to a 200 $\mu$m × 200 $\mu$m size synchrotron X-ray beam with 0.7653 Å wavelength and the scattering pattern was recorded using a high-resolution image detector (Mar 3450). The XRD patterns were analysed using 'Fit2D' software.

## 3. Results and discussion

Table 1 summarises the thermal transitions and their associated thermodynamic parameters of compounds **1–14**, as determined by DSC and TGA. Compound **1** had a crystal-to-liquid transition ($T_m$) at 178.4 ($\Delta H$ = 154.4 J $g^{-1}$) and 177.9°C ($\Delta H$ = 147.1 J $g^{-1}$) in its first and second heating cycles. Correspondingly, there was an exotherm in each of the cooling cycles due to crystallisation. Compound **2** also exhibited a large endotherm in each of the heating cycles, which corresponded to its $T_m$ at 130.3 ($\Delta H$ = 128.1 J $g^{-1}$) and 129.8°C ($\Delta H$ = 120.2 J $g^{-1}$), respectively. However, in each of the cooling cycles, there were three exotherms. POM studies indicated that it presumably had a monotropic LC phase of the mesophase range of 9 °C, since it developed a Schlieren texture of a LC phase on cooling from the isotropic liquid phase. In this regard, the monotropic property, which is the unstable mesophase of this compound, is in sharp

Table 1. Thermal transitions and their associated thermodynamic parameters of **1–14**.

| Compound | $T_g$[e] (°C) | $T_m$[a] (°C) ($\Delta H$ in J $g^{-1}$) | $T_i$[c] (°C) ($\Delta H$ in J $g^{-1}$) | $\Delta T$[d] (°C) | $T_d$[b] (°C) |
|---|---|---|---|---|---|
| 1 | | 1H 178.4 (154.4) | | | 307 |
| 2 | | 1H 130.3 (128.1) *1C 91.0 (–95.2), 102.8 (–2.9) | 111.8 (–15.4) | | 342 |
| 3 | | 1H 295.1 (120.7) | | | 400 |
| 4 | | 1H 267.1 (120.6) | 294.6 (6.8) | 29 | 397 |
| 5 | | 1H 224.3 (114.6) | 247.0 (3.2) | 23 | 397 |
| 6 | | 1H 248.0 (144.5) *1C 215(–124.8) | 245.0 (–1.9) | | 394 |
| 7 | | 1H 212.8 (110.2) | 219.6 (1.4) | 7 | 385 |
| 8 | | 1H 183.2 (50.1) | 191.3 (0.6) | 8 | 395 |
| 9 | | 1H 196.8 (13.2)[f], 221.6 (1.2)[f], 247.5 (77.8) | | | 364 |
| 10 | 2H 56.8 | 1H 175.3 (3.7)[f], 189.8 (81.2) | | | 367 |
| 11 | 2H 37.4 | 1H 115.8 (70.8) | | | 381 |
| 12 | 2H 61.8 | 1H 201.5 (85.9) | | | 380 |
| 13 | 2H 49.4 | 1H 222.5 (114.3) | | | 367 |
| 14 | 2H 40.0 | 1H 130.5 (73.0) | | | 384 |

*Monotropic liquid-crystalline phase.
[a]$T_m$ = crystal-to-liquid or crystal-to-liquid crystal transition.
[b]$T_d$ = decomposition temperature at which a 5% weight loss of a compound occurred with a heating rate of 10°C $min^{-1}$ in nitrogen.
[c]$T_i$ = liquid crystal-to-liquid transition.
[d]$\Delta T = T_i - T_m$.
[e]$T_g$ = glass transition temperature recorded from the second heating cycle.
[f]Crystal-to-crystal transition.

contrast to another series of azomethine compounds (reversed azomethine linkage), prepared from condensation reactions of $\alpha,\omega$–bis(4-formyl)phenyl-4′-oxy alkanes and 4-n-alkylanilines, which exhibit a rich smectic polymorphism phenomenon (*2*).

Compound **3**, like compound **1**, had an essentially identical $T_m$ at 295.1 with $\Delta H = 120.7$ J g$^{-1}$ and $\Delta H =$ 115.7 J g$^{-1}$ in its first and seconding heating cycles, respectively. Correspondingly, there were crystallisation exotherms at 277.9 ($\Delta H$ = 118.3 J g$^{-1}$) and 272.6°C ($\Delta H = 119.7$ J g$^{-1}$) in its cooling cycles from the isotropic liquid phase. In contrast, compound **4** showed two endotherms at 267.1 ($\Delta$H = 120.6 J g$^{-1}$) and 296.4°C ($\Delta H = 6.8$ J g$^{-1}$) in the first heating cycle and two exotherms at 292.7 ($\Delta H$ = 119.4 J g$^{-1}$) and 249.75°C ($\Delta H = 8.5$ J g$^{-1}$) in the first cooling cycle. In the second heating cycle, it showed essentially identical endotherms with identical enthalpy changes to those in the first heating cycle. Similarly, two exotherms and enthalpy changes associated with these transitions in the second cooling cycle were essentially identical to those in the first cooling cycle. Note here that the low-temperature endotherm underwent a high degree of supercooling of 17.3°C and the high-temperature endotherm underwent a low degree of supercooling of 2.3°C. In addition, its enthalpy change for the high-temperature endotherm was much lower than that of the low-temperature endotherm, which was indicative of a nematic LC phase present in this compound. In conjunction with POM studies it was confirmed that the low-temperature endotherm was related to its crystal-to-LC phase ($T_m$) transition and the high-temperature endotherm to its LC-to-isotropic phase ($T_i$) transition. Therefore, it had a mesophase range of 29.3°C. The optical texture developed in its LC phase on melting, as studied by POM, contained a typical Schlieren texture or a threaded texture. In addition, there was a development of a droplets texture when it was cooled from the isotropic liquid phase. Such droplets are, as shown in Figure 1(a), characterise uniquely the nematic phase of this compound, since they occur in no other LC phases (*16–19*). Figure 2 shows the DSC thermograms of compound **5** taken at heating and cooling rates of 10°C min$^{-1}$ in nitrogen. Similar to compound **4**, it exhibited two endotherms in its first heating cycle and two exotherms in its first cooling cycle, albeit with decreased enthalpy changes associated with these transitions in both the cycles. Its endotherms in the second heating cycle were essentially identical to those in the first heating cycle; its exotherms in the second cooling cycle were also essentially identical to those in the first cooling cycle. The low-temperature endotherm was related to $T_m$ at 224.3°C with $\Delta H =$ 114.6 J g$^{-1}$ and the high-temperature endotherm to its

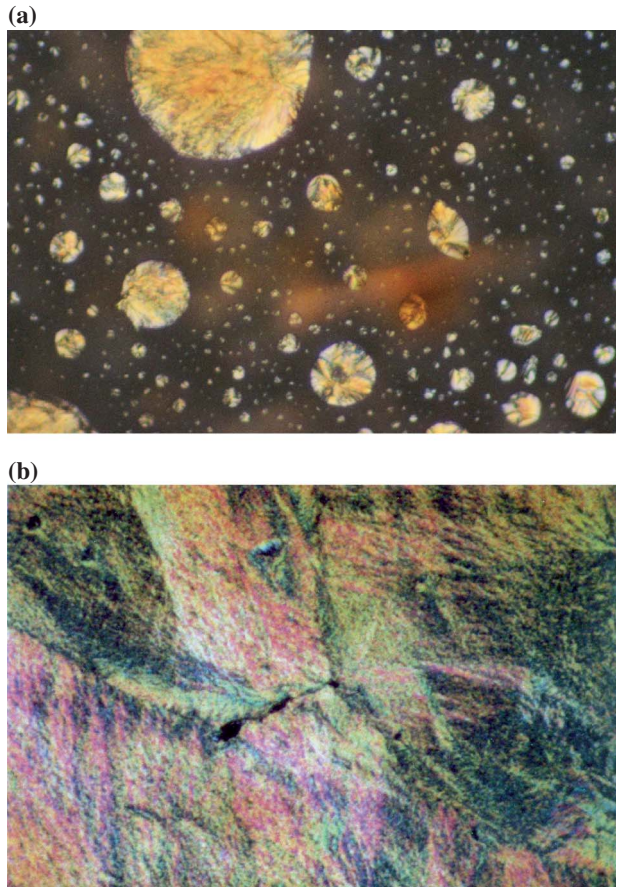


Figure 1. Photomicrographs (a) and (b) of compounds **4** and **5**, respectively, under crossed polarisers taken on cooling from their isotropic phase displaying a nematic LC phase (magnification 400×).

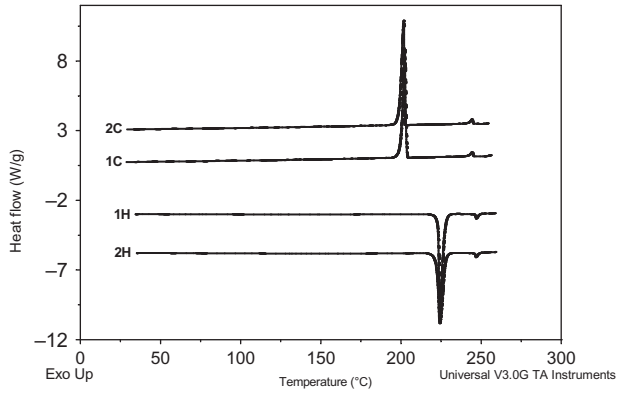


Figure 2. DSC thermograms of compound **5** obtained at heating and cooling rates of 10°C min$^{-1}$ in nitrogen.

$T_i$ at 247.0°C with $\Delta H = 3.2$ J g$^{-1}$. Therefore, it showed a slightly lower mesophase range of 22.7°C, since the odd-numbered nine methylene units present in this compound, when compared with the even-numbered

six methylene units present in compound **4**, not only decreased the $T_m$, but also the $T_i$, resulting in a lower range of mesophases. The optical texture developed in its LC phase on melting, as studied by POM as in compound **4**, also contained a typical Schlieren texture or threaded texture, as shown in Figure 1(b), suggesting its nematic LC phase. In contrast to compounds **4** and **5**, compound **6** exhibited a single, sharp endotherm at 248°C with $\Delta H = 114.5$ J g$^{-1}$ in the first heating cycle, but two exotherms at 245°C with $\Delta H = 114.6$ J g$^{-1}$ and 215°C in $\Delta H = 2.0.6$ J g$^{-1}$ in the first cooling cycle (not shown). All of these transitions were also reproducible, both in the second heating and cooling cycles with slightly decreased enthalpy changes. All of these thermograms were indicative of a monotropic LC phase, that is, it had a mesophase range of 30°C in the cooling cycles only. The LC phase present in this compound was also found to be nematic, because of both the low enthalpy change associated with the transformation from the liquid-to-LC phase transition and the development of a marbled texture on cooling as shown in Figure 3(a).

Figure 4 shows the DSC thermograms of compound **7** obtained at heating and cooling rates of 10°C min$^{-1}$ in nitrogen. It clearly exhibited two endotherms (one large at 212.8°C with $\Delta H = 114.6$ J g$^{-1}$ and one small at 219.7°C with $\Delta H = 1.4$ J g$^{-1}$) in the first heating cycle. However, it showed three exotherms (one large and two small) in the first cooling cycle. All of these transitions were reproducible both in the second heating and cooling cycles with somewhat decreased enthalpy changes associated with these transitions. The high-temperature, small exotherm underwent a low degree of supercooling that suggested its transition from isotropic liquid to the LC phase transition. The other small and large exotherms underwent a high degree of supercooling in the thermograms, which suggested that they were associated with crystallisation exotherms, since a LC-to-LC phase transition and the isotropic liquid-to-LC phase usually undergo little or no supercooling. This compound had a low mesophase range ca. 7°C, but it was enantiotropic in nature in contrast to compound **6**. The LC texture of this compound, as shown Figure 3(b), suggested that it also exhibited a nematic LC phase. DSC thermograms of compound **8** (not shown) showed its $T_m$ at 183.2°C with $\Delta H = 50.1$ J g$^{-1}$ and $T_i$ at 191.3°C with $\Delta H = 0.6$ J g$^{-1}$ in both the heating cycles, thus resulting in a mesophase range of ca. 8°C. It also exhibited an enantiotropic LC phase and the nature of the LC phase was found to be nematic, since it developed a typical marbled texture (not shown). These results (*vide supra*) for the development of a nematic LC phase in compounds **4**–**8** are in excellent agreement with those of analogous series

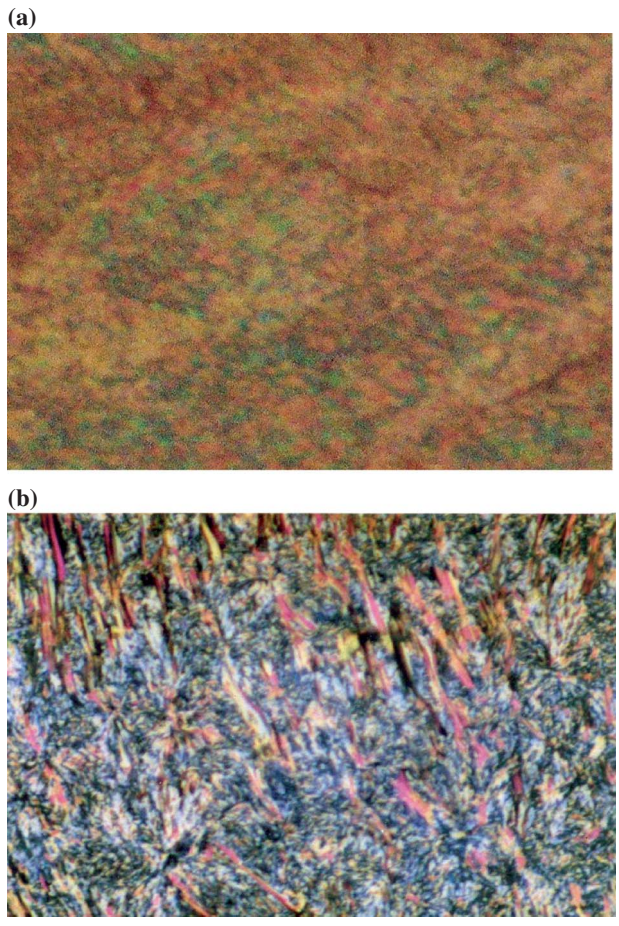


Figure 3. Photomicrographs (a) and (b) of compounds **6** and **7**, respectively, under crossed polarisers taken on cooling from their isotropic phase displaying a nematic LC phase (magnification 400×).

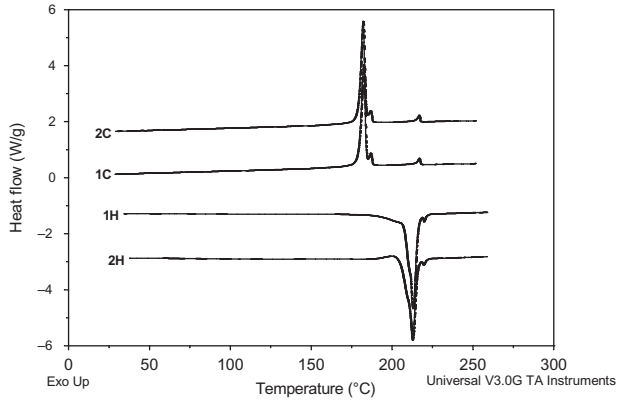


Figure 4. DSC thermograms of compound **7** obtained at heating and cooling rates of 10°C min$^{-1}$ in nitrogen.

of azomethine dimers as reported by Henderson *et al.* (*4*) and Imrie and Henderson (*20*).

Compound **9**, containing anthracene moieties and recrystallised from DMF, showed two small

endotherms in the low-temperature region (a crystal–crystal transition as verified with POM studies) and a large endotherm at 247.5°C with $\Delta H = 77.8$ J g$^{-1}$ in the first heating cycle. It also exhibited a broad, crystallisation exotherm at 171.3°C with $\Delta H = -58.0$ J g$^{-1}$, which underwent a high degree of supercooling because of the difficulty in the packing of this molecule for crystallisation. In the second heating cycle, there was only a cold crystallisation exotherm and a large endotherm at 247.0°C with the increased $\Delta H = 80.0$ J g$^{-1}$. This large endotherm was related to its crystal-to-liquid ($T_m$) transition. Compound **10**, recrystallised from DMF, also exhibited a small endotherm at 175°C and a large endotherm at 189.8°C with $\Delta H = 81.2$ J g$^{-1}$. In the first cooling cycle, there was no crystallisation exotherm, which suggested that it did not crystallise at the experimental conditions used. In the second heating cycle, it showed a glass transition ($T_g$) at 56.8°C, a broad cold crystallisation exotherm and a large endotherm at 188.4°C with increased $\Delta H = 86.6$ J g$^{-1}$. In the second cooling, there was also no crystallisation exotherm. VTXRD and POM studies confirmed that this compound did not exhibit LC phases, but its crystallinity surprisingly increased with the increase in temperature up to the $T_m$, at which it transformed into an isotropic liquid phase, as evident from the XRD patterns. In POM studies, the highly birefringent textures of different polymorphic crystal structures were also observed (Figure 5(a)). Compound **11**, recrystallised from DMF, exhibited one large endotherm in its first heating cycle irrespective of the heating rates of 1, 5, 10, and 20°C min$^{-1}$. The peak maxima for all these endotherms were 111.6, 114.5, 115.8 and 117.5°C with $\Delta$H values in the range of 69.6–75.2 J g$^{-1}$, which corresponded to its melting transition that was slightly dependent on the heating rates used. In the cooling cycle, there was a single $T_g$ at all cooling rates tested. Therefore, it could not be crystallised on melting even at the slowest cooling rate of 1°C min$^{-1}$. In the second heating cycle, it also exhibited a single $T_g$ but no melting endotherm. Its $T_g$ values were in the range of 37.4–39.6°C as determined at various heating rates. Compound **12**, recrystallised from DMF, showed a sharp melting endotherm at 201.5°C with $\Delta H = 85.9$ J g$^{-1}$ in the first heating cycle. On subsequent cooling, it showed a single $T_g$ at 60.9°C. In the second heating cycle, it also showed a single $T_g$ at 61.8°C, but no melting endotherm. On melting it formed a glassy phase under the experimental conditions used. Figure 6 shows the DSC thermograms of compound **13**, recrystallised from DMF, obtained at heating and cooling rates of 10°C min$^{-1}$ in nitrogen. In its first heating cycle, there was a weak crystallisation exotherm, a small endotherm at 204.2°C with $\Delta H =$ 1.8 J g$^{-1}$ and a large endotherm at 222.5°C with $\Delta H =$ 114.3 J g$^{-1}$. In the subsequent cooling cycle, the absence of any exotherms and the presence of a weak $T_g$ suggested that it did not crystallise on cooling from its isotropic liquid phase. However, in the second

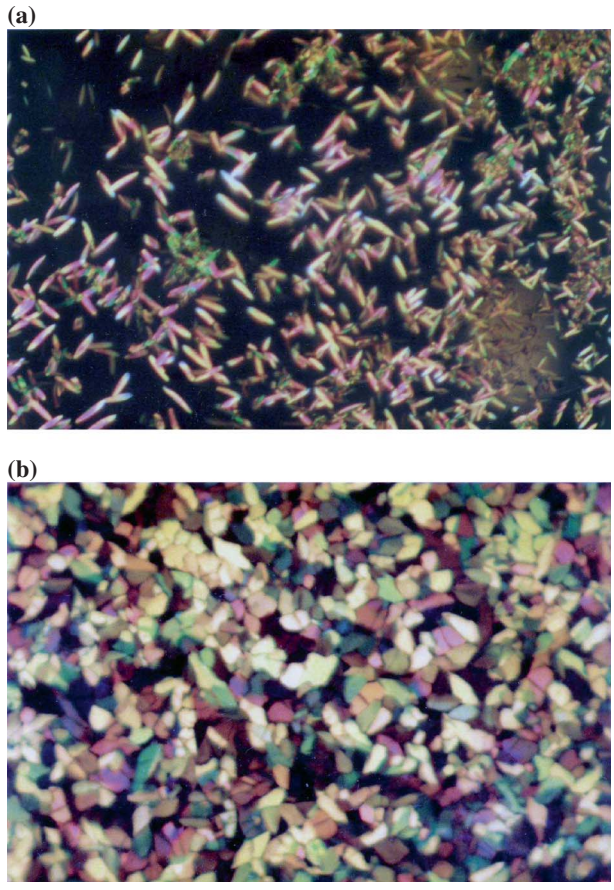


Figure 5. Photomicrographs (a) and (b) of compounds **10** and **13** under crossed polarisers taken at 110 and 220°C, respectively, displaying their crystalline phases (magnification 400×).

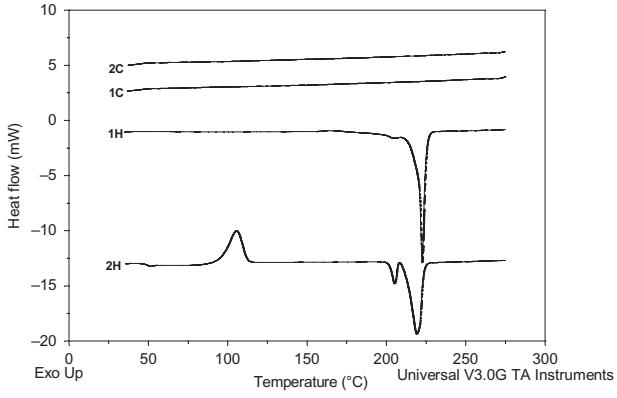


Figure 6. DSC thermograms of compound **13** obtained at heating and cooling rates of 10°C min$^{-1}$ in nitrogen.

heating cycle, its thermogram displayed a $T_g$ at 49.4°C immediately followed by a large, cold crystallisation exotherm, a sharp, small endotherm at 205.0°C with $\Delta H = 15.5$ J g$^{-1}$ and a large endotherm at 219.0°C with $\Delta H = 110.2$ J g$^{-1}$. To understand the nature of these transitions for this compound, we also studied the effect of the heating and cooling rates of 20 and 5°C min$^{-1}$. The main features of these thermograms remained essentially similar to those obtained at heating and cooling rates of 10°C min$^{-1}$ (not shown). However, its $T_g$ values, its peak maxima of two endotherms, and its enthalpy changes associated with these transitions all of which were dependent on the thermal history of this compound. Its VTXRD patterns, shown in Figure 7, suggested that the low-temperature endotherm was related to its polymorphism (crystalline phase) and the high-temperature endotherm was related to the transformation of the crystalline phase to the isotropic liquid phase. It showed a highly crystalline XRD pattern recorded at 210°C (Figure 7(c)), which on further heating at ca. 222°C transformed into an isotropic phase, which contained the typical pattern of diffused both inner and outer rings (Figure 7(d)). The photomicrograph taken at 220°C (Figure 5(b)) also suggested its crystalline phase, but not the LC phase. These results are in excellent agreement with those of a completely architecturally different series of bisstyrylanthracene derivatives, which also exhibit polymorphism, reported by Konishi *et al.* (*21*). Compound **14**, recrystallised from DMF, showed a sharp, melting endotherm at 130.5°C with $\Delta H = 73.0$ J g$^{-1}$ in the first heating cycle. On subsequent cooling, it showed a single $T_g$ at 39.5°C. In the second heating cycle, it also showed a single $T_g$ at 40.0°C, but no melting endotherm. On melting it also formed a glassy phase under the experimental conditions used. These results are in sharp contrast to the results of a series of azomethine compounds (reversed azomethine linkages) prepared from the condensation reactions of α,ω–bis(4-formyl)phenyl-4′-oxy alkanes with 1-aminopyrene, which exhibit



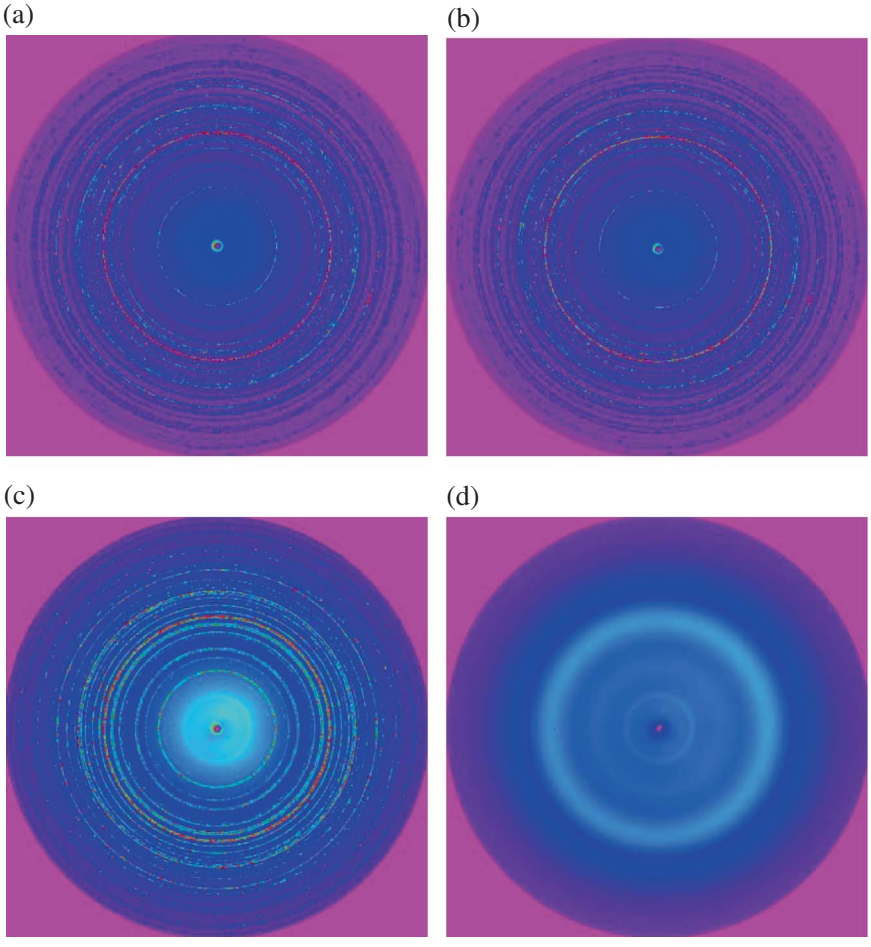


Figure 7. Wide-angle X-ray diffraction patterns of compound **13** taken at (a) 80, (b) 152 and (c) 210°C on heating, exhibiting crystalline phases; and (d) at 240°C on cooling, exhibiting an isotropic liquid phase.

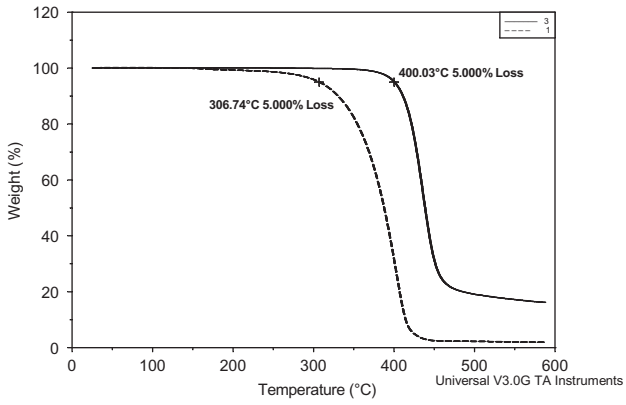


Figure 8. TGA plots of compounds **1** and **3** obtained at a heating rate of 10°C $min^{-1}$ in nitrogen.

either nematic or smectic glasses, depending on the number of methylene units present in their structures (*22*, *23*).

The thermal stabilities of compounds **1**–**14** were determined by TGA in nitrogen at a heating rate of 10°C $min^{-1}$ in nitrogen. The typical TGA plots of **1** and **3** are shown in Figure 8 as representative examples for all of these compounds. The thermal-stability limit is the temperature at which 5% weight loss of a compound occurred. Compounds **1** and **2**, containing phenyl moiety, had relatively low thermal stability of 307 and 342°C, respectively. In contrast, compounds **3**–**8**, containing biphenyl moiety, had the highest thermal stability, which was in the range of 385–400°C. Compounds **9**–**14** had the intermediate range of thermal stability of 364–384°C. When compared with the phenyl moiety present in **1** and **2,** both biphenyl and anthracenyl moieties present in **3**–**14** increased the aromaticity indices in all of these compounds and, therefore, increased the thermal stability significantly, even though some of these compounds contained the weak link of single oxyethlene and oligooxyethlene units. Note here that the aromaticity indices are generally important parameters in determining not only the thermal stability but also the mesogenicity of many organic compounds and polymers (*24*). In general, their high thermal stability permitted one to study their thermal transitions without the interferences of their thermal decompositions.

## 4. Conclusions

We presented the synthesis of a series of azomethine dimers, **1**–**14**, prepared by condensation reactions of benzaldehyde, biphenylcarboxaldehyde and 9-anthraldehyde, with various aromatic diamines of varying flexibility in ethanol in the presence of tosic acid.

Their chemical structures were determined by spectroscopic techniques and elemental analysis. Their thermal properties, including LC properties, were examined by using a number of experimental techniques that included DSC, TGA, POM and VTXRD. For example, compound **2**, prepared from benzaldehyde and BAPN, exhibited a monotropic, nematic LC phase. Compounds **3**–**8**, containing biphenyl moieties, with the exception of **3** and **6**, exhibited an enantiotropic, nematic LC phase with variable ranges of mesophases depending on the flexibility of the aromatic diamines used. Compounds **9**–**14**, containing anthracene moieties, did not exhibit any LC phase, but did show polymorphism as determined in the case of compounds **10** and **13** by POM and VTXRD. All of these anthracene-containing compounds showed varying $T_g$ and $T_m$ values depending on the flexibility of the aromatic diamines used. In addition, they usually formed an amorphous phase on cooling from the isotropic liquid phase and could be useful for optoelectronic devices because of the presence of anthracene moieties. All the compounds in the series had excellent thermal stability that was in the range of 307–400°C.

## Acknowledgements

PKB acknowledges the University of Nevada Las Vegas (UNLV) for the New Investigation Award (NIA), the Planning Initiative Award (PIA) and the Applied Research Initiative (ARI) grants; the donors of the Petroleum Research Fund, administered by the American Chemical Society; and an award (CCSA# CC5589) from the Research Corporation for the support of this research. AKN acknowledges the Graduate College (UNLV) for providing him with a Nevada Stars Graduate Assistantship for the period of 2006–2008. HDM acknowledges Texas A&M International University (TAMIU) for a mini-research grant and the Welch Foundation for a summer research grant (BS0040). Use of Advanced Photon Source (APS) is supported by the U.S. Department of Energy, Basic Energy Sciences, Office of Science, under Contract No. W-31-109-Eng-38. The Midwest Universities Collaborative Access Team's sector at the APS is supported by the U.S. Department of Energy, Basic Energy Sciences, Office of Science, through the Ames Laboratory under Contract No. W-7405-Eng-82. This research is supported, in part, by the National Science Foundation grant DMR-03-12792.

## References

(1) Attard, G.S.; Imrie, C. *Liq. Cryst.* **1992**, *11*, 785–789.
(2) Date, R.W.; Imrie, C.T.; Luckhurst, G.R.; Seddon, J.M. *Liq. Cryst.* **1992**, *12*, 203–238.
(3) Blatch, A.E.; Luckhurst, G.R. *Liq. Cryst.* **2000**, *27*, 775–787.

(4) Henderson, P.A.; Niemeyer, O.; Imrie, C.T. *Liq. Cryst.* **2001**, *28*, 463–472.
(5) Dierking, I. *Textures of Liquid Crystals*; Wiley-VCH: Weinheim, 2003.
(6) Henderson, P.A.; Seddon, J.M.; Imrie, C.T. *Liq. Cryst.* **2005**, *32*, 1499–1513.
(7) Iwan, A.; Sek, D. *Prog. Polym. Sci.* **2008**, *33*, 289–345.
(8) Parra, M.L.; Saavedra, C.G.; Hidalgo, P.I.; Elgueta, E.Y. *Liq. Cryst.* **2008**, *35*, 55–64.
(9) Marin, L.; Destri, S.; Porzio, W.; Bertini, F. *Liq. Cryst.* **2009**, *36*, 21–32.
(10) Parra, M.L.; Elgueta, E.Y.; Jimenez, V.; Hidalgo, P.I. *Liq. Cryst.* **2009**, *36*, 301–317.
(11) Yin, J.; Ye, Y.-F.; Wang, Z.-G. *Eur. Polym. J.* **1998**, *34*, 1839–1843.
(12) Shiotani, A.; Kohda, M. *J. Appl. Polym. Sci.* **1999**, *74*, 2404–2413.
(13) Kricheldorf, H.R.; Linzer V. *Polymer* **1995**, *36*, 1893–1902.
(14) Wagner, E. *J. Prakt. Chem.* **1883**, *27*, 199–230.
(15) Feld, W.A.; Ramalingam, B.; Harris, F.W. *J. Polym. Sci. Polym. Chem. Ed.* **1983**, *21*, 319–328.
(16) Demus, D.; Richter, L. *Textures of Liquid Crystals*; Chemie: Weinheim, 1978.
(17) Kelker, H.; Katz, R. *Handbook of Liquid Crystals*; Chemie: Weinheim, 1980.
(18) Han, H.; Bhowmik, P.K. *J. Polym. Sci. Polym. Chem. Ed.* **1995**, *33*, 211–225.
(19) Han, H.; Bhowmik, P.K. *Prog. Polym. Sci.* **1997**, *22*, 1431–1502.
(20) Imrie, C.T.; Henderson P.A. *Chem. Soc. Rev.* **2007**, *36*, 2096–2124.
(21) Konishi, M.; Fujita, K.; Tsutsui, T. *Mol. Cryst. Liq. Cryst.* **2004**, *425*, 11–19.
(22) Attard, G.S.; Imrie, C.T. *Liq. Cryst.* **1992**, *11*, 785–789.
(23) Attard, G.S.; Imrie C.T.; Karasz, F.E. *Chem. Mater.* **1992**, *4*, 1246–1253.
(24) Dolden, J.G. *Adv. Polym. Sci.* **1999**, *141*, 189–244.